# Supporting Information

for

## Dual Intercalation of Inorganics-organics Synergistically Tuning the Layer Spacing of $V_2O_5 \cdot nH_2O$ Boosts $Zn^{2+}$ Storage for Aqueous Zinc-Ion Batteries

Ziyi Feng, Yifu Zhang*, Yunfeng Zhao, Jingjing Sun, Yanyan Liu, Hanmei Jiang, Miao Cui, Tao Hu*, Changgong Meng*

*State Key Laboratory of Fine Chemicals, School of Chemical Engineering, Dalian University of Technology, Dalian, 116024, China*

*Corresponding authors.
Yifu Zhang: yfzhang@dlut.edu.cn, +86-13654946624
Tao Hu: inorchem@dlut.edu.cn
Changgong Meng: cgmeng@dlut.edu.cn

## Experimental section

### *Materials preparation*

All the chemicals with analytical pure were used directly without any further purification. The synthetic process of $Mg_xV_2O_5\cdot nH_2O$/PANI (denoted as MgVOH/PANI) is shown in Figure 1a. Firstly, 1 mmol $V_2O_5$ powder was dissolved in 30 mL deionized water at room temperature under vigorous magnetic stirring. And then 1 mL of $H_2O_2$ (30 wt.%) was added into the solution slowly. After obtaining a clear orange-red solution, 1 mmol of $MgCl_2\cdot 6H_2O$ powder and 60 μL of aniline were added into the mixture. Afterward, 3 M HCl was added dropwise to the above mixed solution to adjust the pH value at 3 and the mixture was stirred at room temperature for 30 min. Then the mixed solution was sealed in a 50 mL Teflon-lined stainless-steel autoclave and further maintained at 120 °C for 24 h. After cooling to room temperature, the dark green precipitates were collected by suction filtration and washed with deionized water for three times. Finally, the precipitates were freeze dried for 48 hours, and the product MgVOH/PANI was obtained. To compare, the products of $V_2O_5\cdot nH_2O$ (denoted as VOH), $Mg_xV_2O_5\cdot nH_2O$ (MgVOH) and $V_2O_5\cdot nH_2O$/PANI (VOH/PANI) were synthesized in the same steps and processes in the absence of $Mg^{2+}$ and aniline source.

### *Characterizations*

X-ray diffraction (XRD) patterns were measured using Panalytical X' Pert powder diffractometer at 40 kV and 40 mA with Ni-filtered Cu Kα radiation. The morphology and size of the as-prepared samples were displayed by field emission scanning electron microscopy (FE-SEM, NOVA NanoSEM 450, FEI) and transmission electron microscopy (TEM, FEITecnai F30, FEI). The as-prepared samples were gold-sputtered in advance before TEM observation, and pretreated with ultrasonication so that it could be dispersed in anhydrous ethanol before TEM observation. Energy-dispersive X-ray spectrometer (EDS) and elemental mapping were obtained by a scanning electron microscope (SEM, QUANTA450). X-ray photoelectron spectra (XPS) was collected through an ESCALAB 250Xi electron spectrometer with an excitation source of Al Kα X-ray radiation and the pass energy is 20 eV. The functional groups' stretching and bending information of the samples was characterized by Fouriertransform infrared spectroscopy (FTIR) and recorded on a Nicolet 6700 spectrometer from 4000 to 400 $cm^{-1}$ with a resolution of 4 $cm^{-1}$. Thermo Scientific spectrometer was used to obtain the chemical bond information by Raman spectrum, with a 532 nm-excitation line. Thermogravimetry analysis (TGA) was conducted on a MTC1000 thermal analysis system from 50 to 1200 °C with a heating rate of 5 °C·min$^{-1}$ under an air atmosphere.

*Electrochemical measurements*

The electrochemical properties were carried out via stainless steel CR2032 coin-type cells. For the electrode preparation, the cathode electrodes were fabricated by mixing 70 wt.% of active material, 20 wt.% of acetylene black, and 10 wt.% of polyvinylidene fluoride (PVDF) binder in N-methyl-2-pyrroli-done (NMP) and coating the slurry onto titanium foil. And then they were dried under vacuum at 60 °C for 9 h. The coin-type cells were assembled by the above cathodes, Zn metal as the anode, 80 μL of 3 M zinc trifluoromethanesulfonate ($Zn(CF_3SO_3)_2$, 98%) aqueous solution as the electrolyte, and a glass fiber filter was used as the separator. The electrochemical performances of the Zn// MgVOH/PANI cells were measured in the voltage range of 0.2-1.5 V (vs. $Zn^{2+}/Zn$). The cyclic voltammetry (CV) and electrochemical impedance spectroscopy (EIS) were conducted using the CHI-660D electrochemical working station. The galvanostatic and intermittent titration technique (GITT) and the galvanostatic charge-discharge (GCD) test were taken in a multichannel battery testing system (LAND CT201A) to analyze the reaction and diffusion kinetics and capacity properties, respectively. All the electrochemical characterizations were carried out at room temperature.

*Theoretical calculation method*

All the geometric optimizations, single-point energies and electronic structures calculations are performed through the spin-polarized density functional theory method by using the Cambridge Serial Total Energy Package (CASTEP) code on the basis of the plane-wave pseudopotential. The Perdew-Burke-Ernzerhof (PBE) exchange-correlation functional for generalized gradient approximation (GGA) and the projector augmented wave (PAW) method explaining the core-valence interactions are employed. The valence electrons were expanded in a plane-wave basis set within a cutoff energy of 500 eV. The electronic relaxation is performed to within an energy tolerance of $2\times10^{-6}$ eV for self-consistency, while ionic optimizations are performed until all the residual forces are smaller than 0.01 eV/Å. Monkhorst-Pack meshes with 2×2×1 and 3×2×1 k-points were used to sample the Brillouin zone of the 3×1×1 MgVOH/PANI super-cell and 2×1×1 $V_2O_5$ super-cell calculations, respectively. Considering the strong on-site Coulombic interactions of V 3d-electrons, we set the effective parameter U=2.5V. Spin-polarized wave functions are used for all calculations. Other than these, we have set a vacuum region of 15 Å along the z-direction to avoid interactions between adjacent images.

**Figure S1**

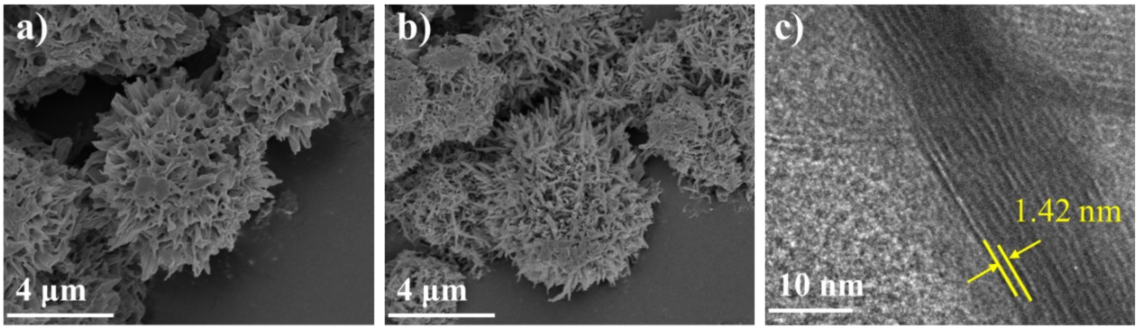

Fig. S1. SEM images of (a) MgVOH and (b) VOH/PANI; (c) HRTEM of MgVOH/PANI.

## Figure S2

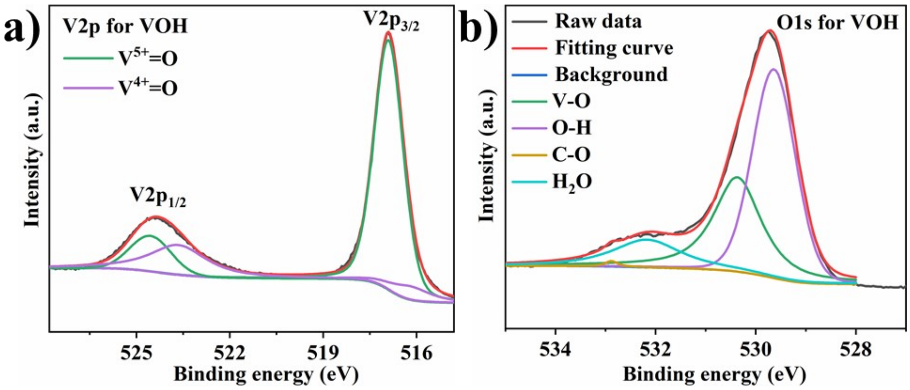

Fig. S2. High resolution XPS spectra of VOH.

## Figure S3

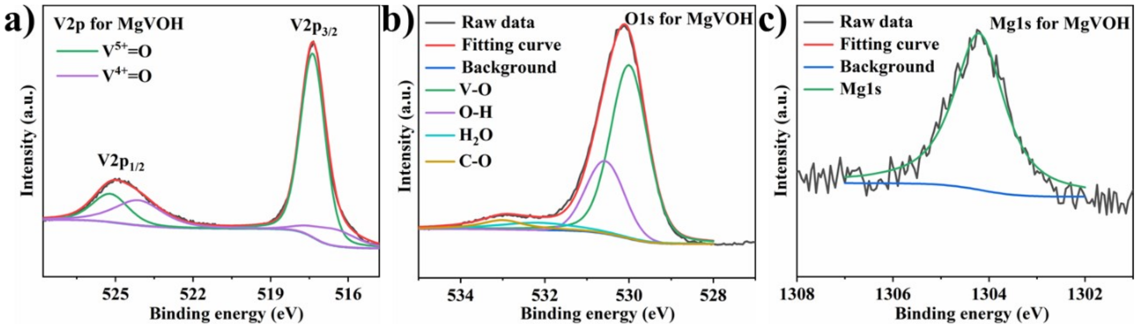

Fig. S3. High resolution XPS spectra of MgVOH.

**Figure S4**

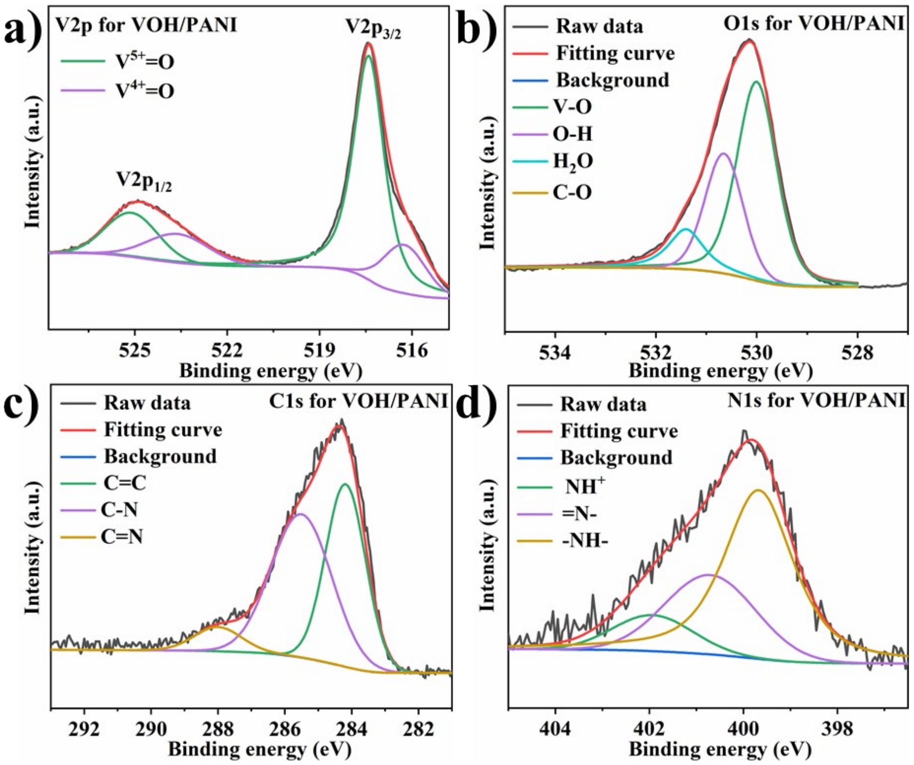

Fig. S4. High resolution XPS spectra of VOH/PANI.

**Figure S5**

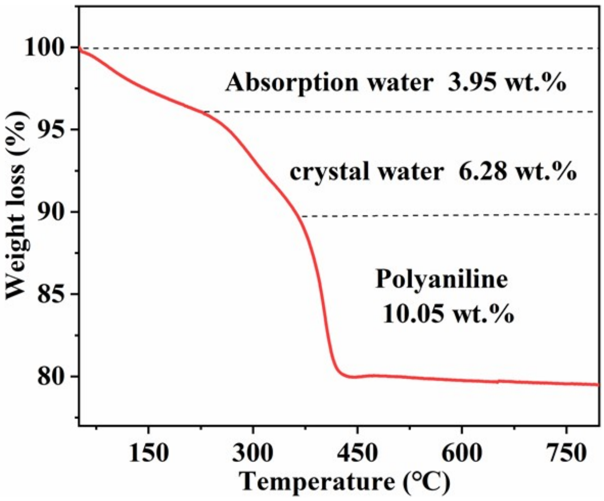

Fig. S5. TGA result of MgVOH/PANI composite.

**Table S1**

**Table S1.** Atomic content of Mg, V, O, C and N in MgVOH/PANI by XPS analysis.

| **Element** | **Atomic%** |
|---|---|
| **Mg** | **0.8** |
| **V** | **17.7** |
| **O** | **49.01** |
| **C** | **28.22** |
| **N** | **4.27** |

**Table S2**

**Table S2.** Atomic content of Mg and V in MgVOH/PANI by ICP analysis.

| **Element** | **Atomic%** |
|---|---|
| **Mg** | **1** |
| **V** | **8** |

**Figure S6**

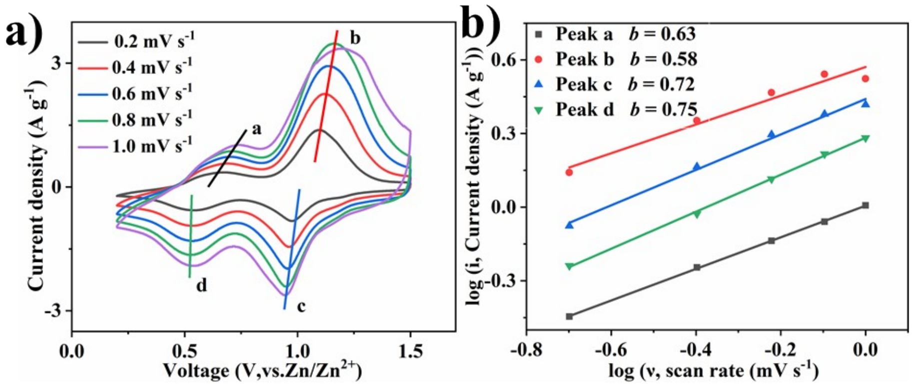

Fig. S6. CV curves at various sweep rates and the relationship between peak currents and sweep rates of VOH.

**Figure S7**

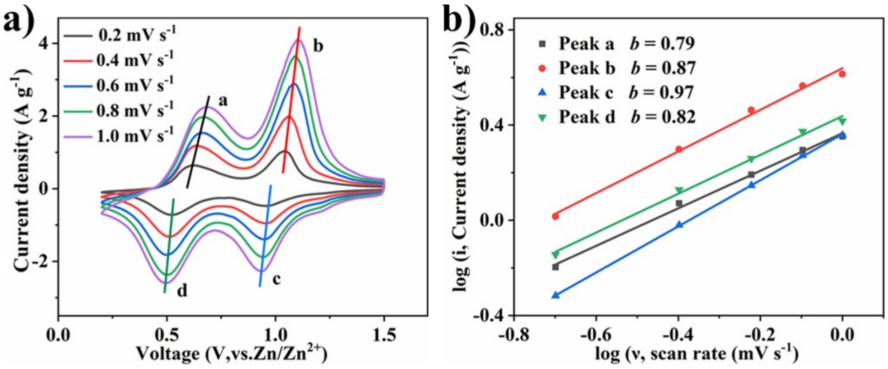

Fig. S7. CV curves at various sweep rates and the relationship between peak currents and sweep rates of MgVOH.

**Figure S8**

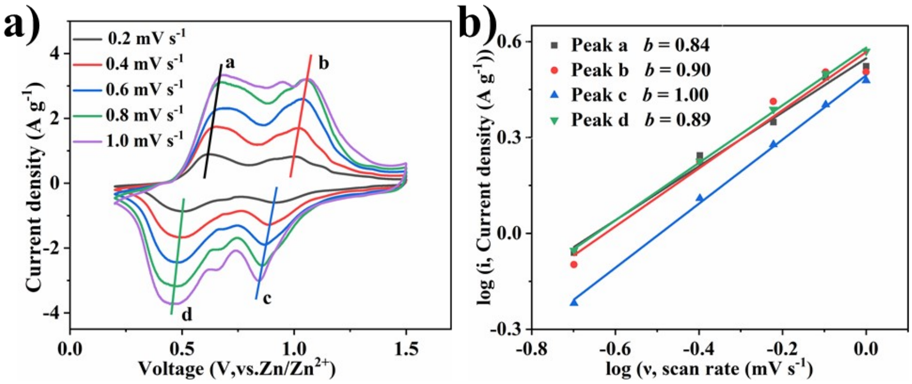

Fig. S8. CV curves at various sweep rates and the relationship between peak currents and sweep rates of VOH/PANI.

**Figure S9**

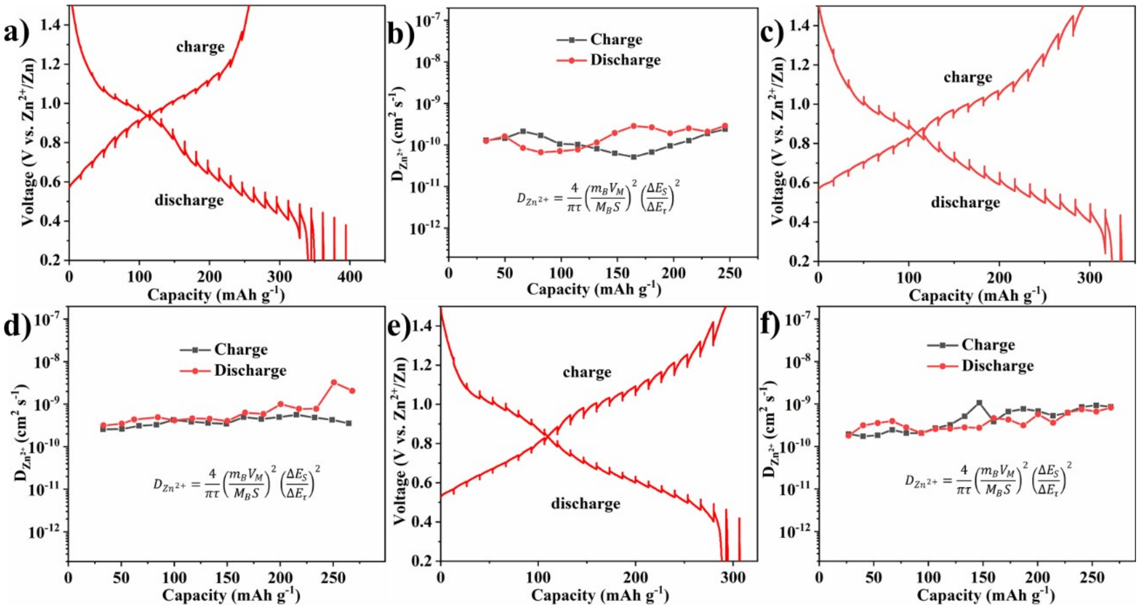

$$D_{Zn^{2+}} = \frac{4}{\pi\tau}\left(\frac{m_B V_M}{M_B S}\right)^2\left(\frac{\Delta E_S}{\Delta E_\tau}\right)^2$$

Fig. S9. GITT curve of (a) VOH, (c) MgVOH and (e) VOH/PANI; the calculated diffusivity coefficient of $Zn^{2+}$ ($D_{Zn2+}$) of (b) VOH, (d) MgVOH and (f) VOH/PANI.

**Figure S10**

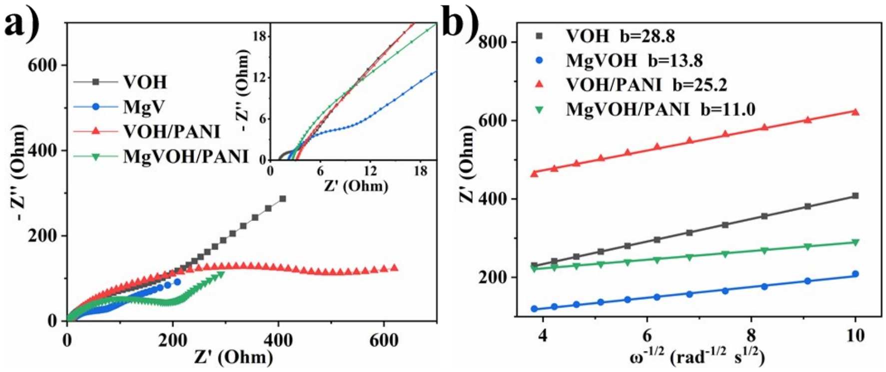

Fig. S10. (a) EIS spectra of VOH, MgVOH, VOH/PANI and MgVOH/PANI; (b) Nyquist plots after different discharge/charge processes of VOH, MgVOH, VOH/PANI and MgVOH/PANI.

**Figure S11**

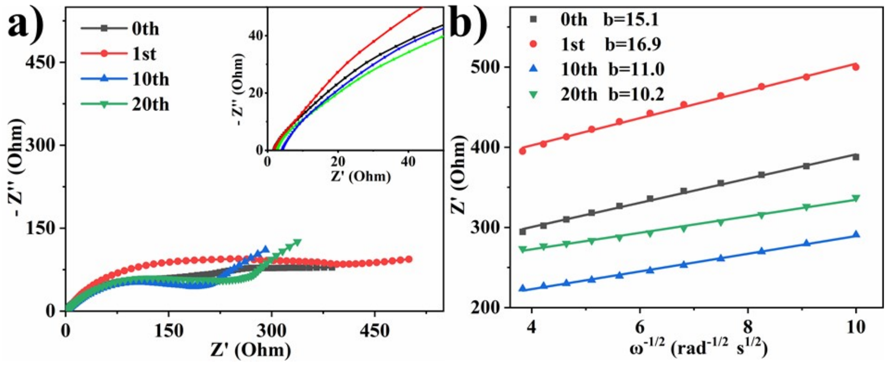

Fig. S11. (a) EIS spectra of MgVOH/ PANI; (b) The slopes of the Nyquist plot of Zn//MgVOH/PANI battery at low frequencies.

**Figure S12**

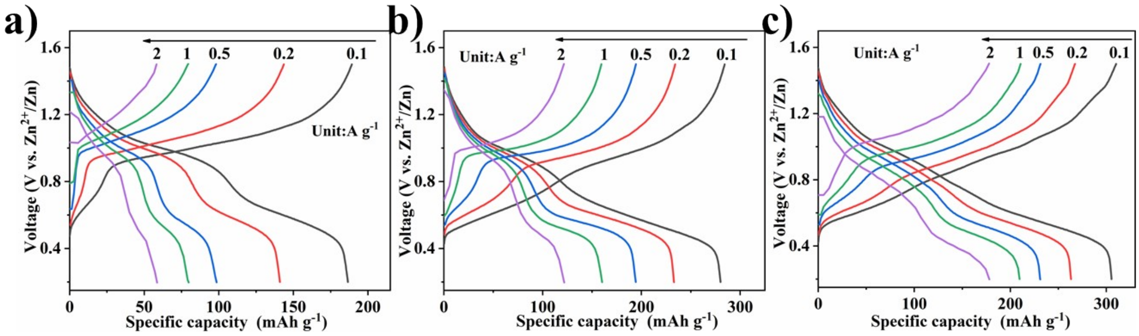

Fig. S12. GCD curves of (a)VOH, (b) MgVOH and (c) VOH/PANI.

**Figure S13**

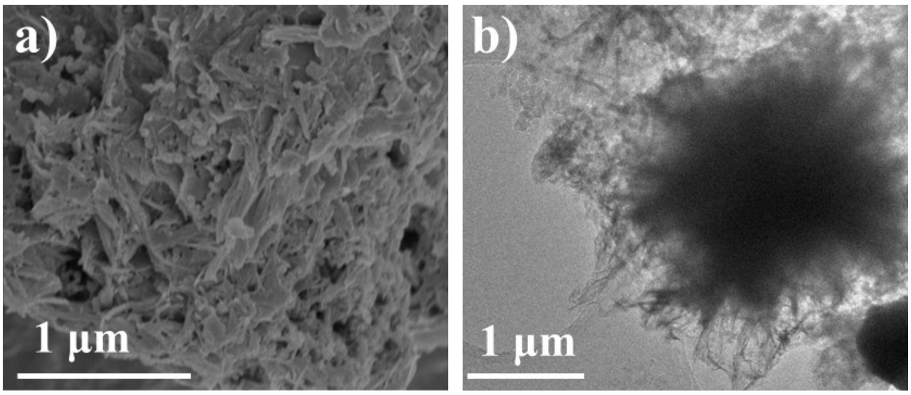

Fig. S13. (a) SEM and (b) TEM images of MgVOH/PANI after a long-term cycle.

**Figure S14**

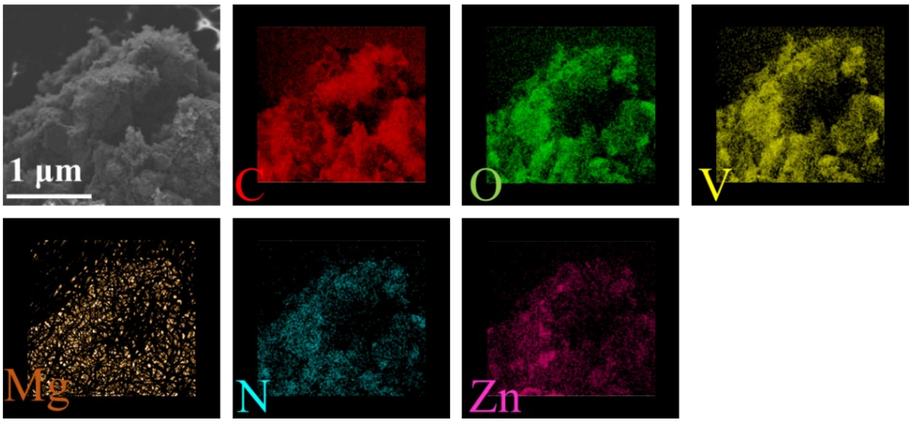

Fig. S14. EDS mapping of MgVOH/PANI after a long-term cycle.

**Figure S15**

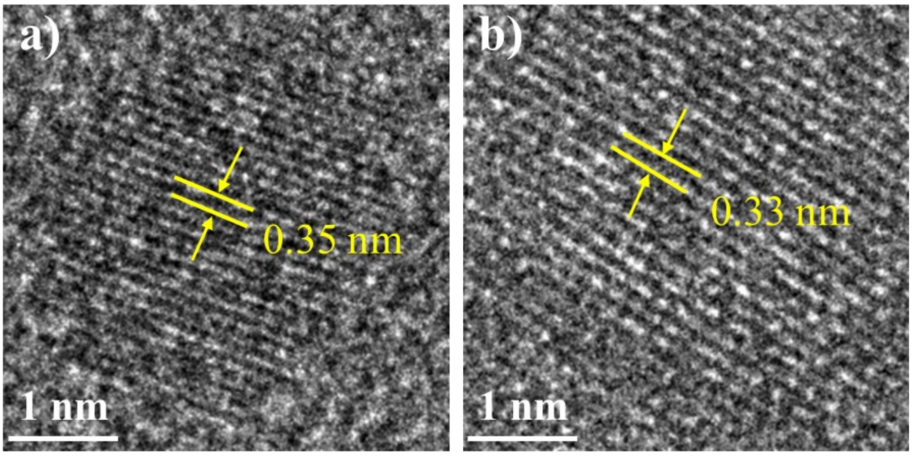

Figure S15. HRTEM of the MgVOH/PANI in the (a) the fully discharged state and (b) the fully charged.

**Figure S16**

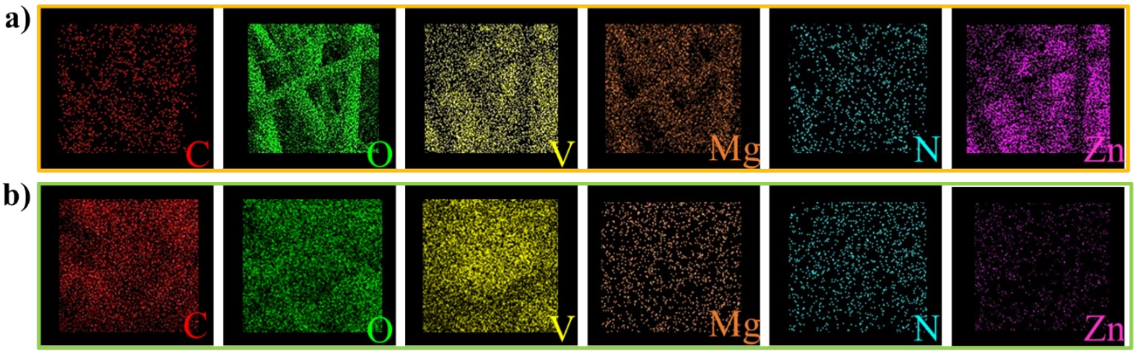

Figure S16. EDS mapping of MgVOH/PANI in the (a) the fully discharged state and (b) the fully charged state.

**Figure S17**

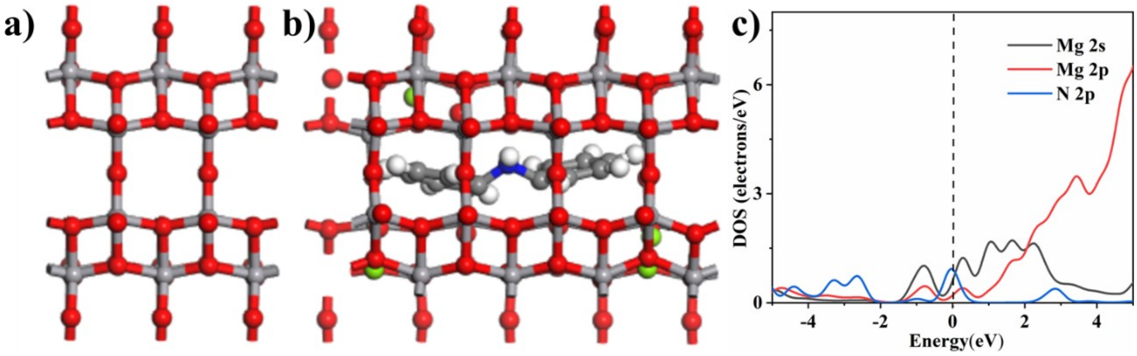

Figure S17. Top (upper panel) view for (a) V2O5 and (b) MgVOH/PANI; (c) the partial densities of states for MgVOH/PANI.